



Deposited via The University of Leeds.

White Rose Research Online URL for this paper:

<https://eprints.whiterose.ac.uk/id/eprint/114223/>

Version: Accepted Version

---

**Article:**

Pritchard, VE, Martir, DR, Oldknow, S et al. (2017) Homochiral self-sorted and emissive Ir(III) metallo-cryptophanes. *Chemistry - A European Journal*, 23 (26). pp. 6290-6294.  
ISSN: 0947-6539

<https://doi.org/10.1002/chem.201701348>

---

**Reuse**

Items deposited in White Rose Research Online are protected by copyright, with all rights reserved unless indicated otherwise. They may be downloaded and/or printed for private study, or other acts as permitted by national copyright laws. The publisher or other rights holders may allow further reproduction and re-use of the full text version. This is indicated by the licence information on the White Rose Research Online record for the item.

**Takedown**

If you consider content in White Rose Research Online to be in breach of UK law, please notify us by emailing [eprints@whiterose.ac.uk](mailto:eprints@whiterose.ac.uk) including the URL of the record and the reason for the withdrawal request.

# Homochiral self-sorted and emissive Ir(III) metallo-cryptophanes

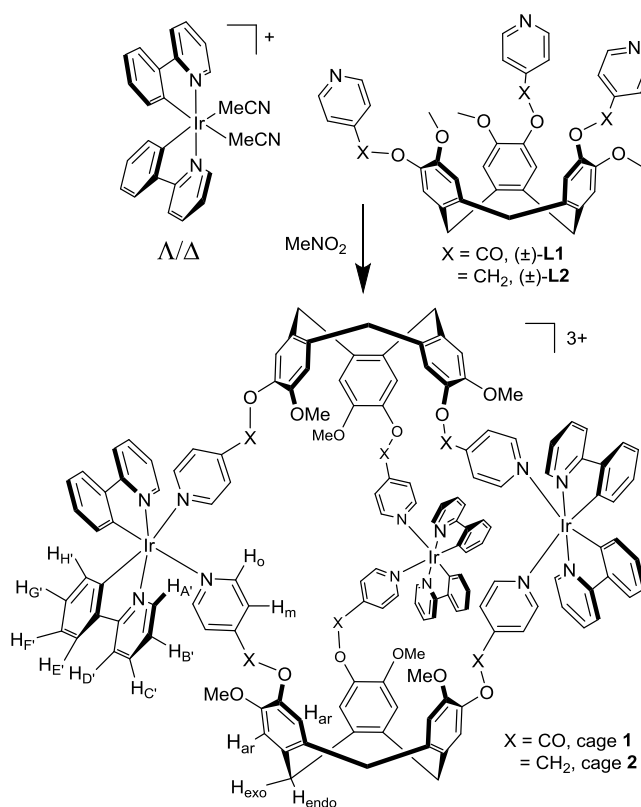
Victoria E. Pritchard,<sup>[a]</sup> Diego Rota Martir,<sup>[b]</sup> Samuel Oldknow,<sup>[a]</sup> Shumpei Kai,<sup>[c]</sup> Shuichi Hiraoka,<sup>[c]</sup> Nikki J. Cookson,<sup>[a]</sup> Eli Zysman-Colman\*,<sup>[b]</sup> and Michael J. Hardie\*<sup>[a]</sup>

Dedicated to the memory of Dr Julie Fisher.

**Abstract:** The racemic ligands ( $\pm$ )-*tris*(isonicotinoyl)-cyclotriguiacylene (L1), or ( $\pm$ )-*tris*(4-pyridyl-methyl)-cyclotriguiacylene (L2) assemble with racemic ( $\Lambda,\Delta$ )-[Ir(ppy)<sub>2</sub>(MeCN)<sub>2</sub>]<sup>+</sup> where ppy = 2-phenylpyridinato to form [[Ir(ppy)<sub>2</sub>]<sub>3</sub>(L)<sub>2</sub>]<sup>3+</sup> metallo-cryptophane cages. The crystal structure of [[Ir(ppy)<sub>2</sub>]<sub>3</sub>(L1)<sub>2</sub>]<sup>3+</sup>·3BF<sub>4</sub> has *MM- $\Lambda\Lambda\Lambda$*  and *PP- $\Delta\Delta\Delta$*  isomers, and homochiral self-sorting occurs in solution, a process accelerated by a chiral guest. Self-recognition between L1 and L2 within cages does not occur, and cages show very slow ligand-exchange. Both cages are phosphorescent, with [[Ir(ppy)<sub>2</sub>]<sub>3</sub>(L2)<sub>2</sub>]<sup>3+</sup> having enhanced and blue-shifted emission when compared with [[Ir(ppy)<sub>2</sub>]<sub>3</sub>(L1)<sub>2</sub>]<sup>3+</sup>.

Metallo-cages are discrete 3-D coordination assemblies with a hollow interior with applications as hosts and nanoscale vessels.<sup>[1]</sup> They form through the self-assembly of multidentate ligands with metals, or with metal complexes with controlled available coordination sites (“metallo-tectons”). Luminescent metallo-cages are known,<sup>[2-6]</sup> with most examples exhibiting fluorescence-active ligands,<sup>[2]</sup> alongside rarer examples of cages with pendant metal-complex emissive groups.<sup>[3]</sup> There are very few examples of metallo-cages constructed from inherently phosphorescent structural components.<sup>[4-6]</sup> Cyclometalated Ir(III) complexes bearing either two N-donor ligands or one N<sup>^</sup>N chelating ligand represent an important subclass of phosphorescent materials.<sup>[7]</sup> Lusby et al reported the enantiopure Ir(III) metallo-cage [[Ir(ppy)<sub>2</sub>]<sub>6</sub>(tcb)<sub>4</sub>](OTf)<sub>6</sub> (tcb = 1,3,5-tricyanobenzene)<sup>[4]</sup> which self-assembles, despite the inertness of the d<sup>6</sup> Ir(III) center, as the *C,C-cis-N,N-trans* arrangement of the ppy ligands has a *trans* labilising effect. The cage shows red-shifted emission compared with a monomeric analogue, and enhanced photoluminescence quantum yields ( $\Phi_{\text{PL}}$ ). To date, this is the only report of a 3-D metallo-cage that utilizes [Ir(ppy)<sub>2</sub>] as the sole metal centre, although mixed metal examples are known.<sup>[5]</sup>

We report herein two metallo-cages of the type [[Ir(ppy)<sub>2</sub>]<sub>3</sub>(L)<sub>2</sub>]<sup>3+</sup> where L is a chiral tripodal ligand related to the molecular host cyclotrimeratrylene (CTV). {M(chelate)}<sub>3</sub>L<sub>2</sub> cages with CTV-type ligands are known as metallo-cryptophanes, and most examples feature square planar metals.<sup>[8]</sup> The [[Ir(ppy)<sub>2</sub>]<sub>3</sub>(L)<sub>2</sub>]<sup>3+</sup> cages reported here show homochiral sorting on crystallization and in solution, and slow ligand exchange behavior is observed.



**Scheme 1.** Synthesis of metallo-cryptophane cage species.

Cages [[Ir(ppy)<sub>2</sub>]<sub>3</sub>(L1)<sub>2</sub>]<sup>3+</sup> **1** and [[Ir(ppy)<sub>2</sub>]<sub>3</sub>(L2)<sub>2</sub>]<sup>3+</sup> **2** are formed from nitromethane mixtures of ( $\Lambda,\Delta$ )-[Ir(ppy)<sub>2</sub>(MeCN)<sub>2</sub>]<sup>+</sup>X (X = PF<sub>6</sub><sup>-</sup>, BF<sub>4</sub><sup>-</sup>) and ( $\pm$ )-L1 or ( $\pm$ )-L2 in 3:2 stoichiometry, Scheme 1. Electrospray ionization mass spectrometry (ESI-MS) gives a triply charged *m/z* peak at 983.1120 (cage **1**) or at 955.2853 (cage **2**), along with [[Ir(ppy)<sub>2</sub>]<sub>3</sub>(L)<sub>2</sub>]<sup>3+</sup> and [[Ir(ppy)<sub>2</sub>]<sub>2</sub>(L)<sub>2</sub>]<sup>3+</sup> fragment species (SI Figs. S3, S4). Initial <sup>1</sup>H NMR of [Ir(ppy)<sub>2</sub>(NCMe)<sub>2</sub>]<sup>+</sup>X and L in d<sub>3</sub>-MeNO<sub>2</sub> show considerable broadening of the resonances and chemical shift changes, most saliently the ppy protons *ortho* to the coordinating N (H<sub>A</sub>) and C (H<sub>H</sub>) move upfield and downfield, respectively, and for cage **2** the previously sharp CH<sub>2</sub> bridge singlet of L2 at 5.19 ppm becomes a complex multiplet as free rotation is hindered (Fig. S15). ROESY spectra of **1** and **2**

[a] Dr V. E. Pritchard, S. Oldknow, Dr N. J. Cookson, Prof. M. J. Hardie  
School of Chemistry  
University of Leeds  
Woodhouse Lane, Leeds LS2 9JT, UK  
E-mail: [m.j.hardie@leeds.ac.uk](mailto:m.j.hardie@leeds.ac.uk)

[b] D. Rota Martir, Dr E. Zysman-Colman  
Organic Semiconductor Centre, EaSTCHEM School of Chemistry  
University of St Andrews  
St Andrews, Fife KY16 9ST, UK  
E-mail: [eli.zysman-colman@st-andrews.ac.uk](mailto:eli.zysman-colman@st-andrews.ac.uk)

[c] S. Kai, Prof S. Hiraoka  
Department of Basic Science  
Graduate School of Arts and Sciences  
The University of Tokyo  
3-8-1 Komaba, Meguro-ku, Tokyo 153-8902, Japan

give expected couplings, including between  $H_{H'}$  on the ppy's and the *ortho* pyridyl protons of L (Figs. S8, S16). Diffusion ordered NMR in  $d_3$ -MeNO<sub>2</sub> for **1**·3PF<sub>6</sub> (Fig. S9) gave a hydrodynamic radius of 18.99 Å.

The structure of **1**·3BF<sub>4</sub>·n(MeNO<sub>2</sub>) was confirmed by crystallography, Fig. 1.<sup>[9]</sup> There are two independent cage **1** cations that show minor structural differences. Anions and additional solvent were not located due to significant disorder. Each cage has three pseudo-octahedrally coordinated Ir(III) centers, each with two ppy ligands and the pyridyl groups from two L1 ligands in a *cis* arrangement. The two L1 ligands bridge between three Ir(III) centers. Average torsion angle between *cis* pyridyl groups is 38.04°, typical for [Ir(ppy)<sub>2</sub>(pyridyl)<sub>2</sub>]-type complexes<sup>[10]</sup> with the bowl shape of CTV-type ligands able to accommodate these torsion angles within the cage structure.

Both L1 ligands within each cage **1** are the same enantiomer, giving the chiral *anti*-cryptophane isomer. Each [Ir(ppy)<sub>2</sub>]<sup>+</sup> unit within a cage has the same chirality, such that only the enantiomeric *MM*- $\Lambda\Lambda\Lambda$  and *PP*- $\Delta\Delta\Delta$  cage isomers are observed in the structure. Given the  $\Lambda$  and  $\Delta$  enantiomers of the [Ir(ppy)<sub>2</sub>]<sup>+</sup> moieties and the *M* and *P* enantiomers of the L-types ligands are present in the reaction mixture, there are twelve possible stereoisomers of the cage.

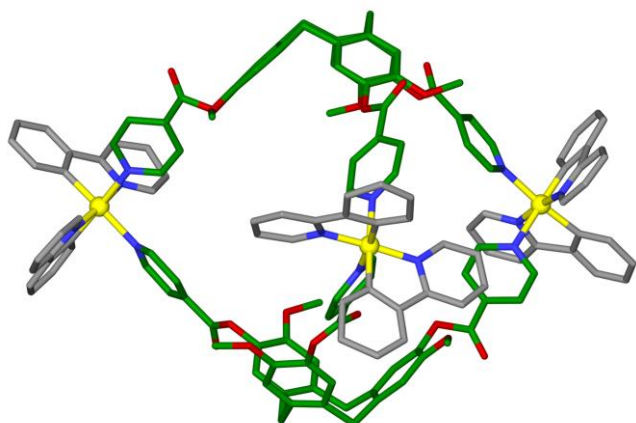


**Figure 1.** A  $[\text{Ir}(\text{ppy})_2]_3(\text{L}1)_2]^{3+}$  cage from the crystal structure of **1**·3BF<sub>4</sub>·n(CH<sub>3</sub>NO<sub>2</sub>), L1 and ppy ligands shown in green and grey respectively.

The <sup>1</sup>H NMR spectra of both cages **1** and **2** undergo significant sharpening upon standing (Figs. S7 and S15), and fully equilibrate after several months. The <sup>1</sup>H NMR spectrum of cage **1**·3PF<sub>6</sub> collected after 3 months of standing is virtually identical to that of the single crystals of **1**·3BF<sub>4</sub>·n(CH<sub>3</sub>NO<sub>2</sub>) re-dissolved in  $d_3$ -MeNO<sub>2</sub>, Fig. 2a/b. ( $\pm$ )-L1 was resolved into its constituent enantiomers by chiral HPLC,<sup>[11]</sup> and each L1 enantiomer reacted with each of  $\Lambda$ -[Ir(ppy)<sub>2</sub>(MeCN)<sub>2</sub>]-BF<sub>4</sub> and  $\Delta$ -[Ir(ppy)<sub>2</sub>(MeCN)<sub>2</sub>]-BF<sub>4</sub>. As expected, two combinations were mismatched pairs of enantiomers that gave poorly resolved <sup>1</sup>H NMR spectra (Figs. S10-11) while two combinations were matched pairs (presumably *M*- $\Delta$  and *P*- $\Lambda$ ) gave sharp spectra in short timeframes that were similar to the fully sorted cage mixture (Figs. 2d, S12-13). ESI-MS of matched and mismatched pairs are similar with all combinations showing cage formation (Fig. S14). The observed <sup>1</sup>H NMR spectral sharpening is therefore indicative of equilibration involving chiral self-sorting of an initial mixture of cage stereoisomers, as was also seen in our previous studies of a [Pd<sub>6</sub>(L1)<sub>8</sub>]<sup>12+</sup> cage but where only the ligand was a chiral

component.<sup>[12]</sup> We could not resolve the sorted cages by analytical chiral HPLC.

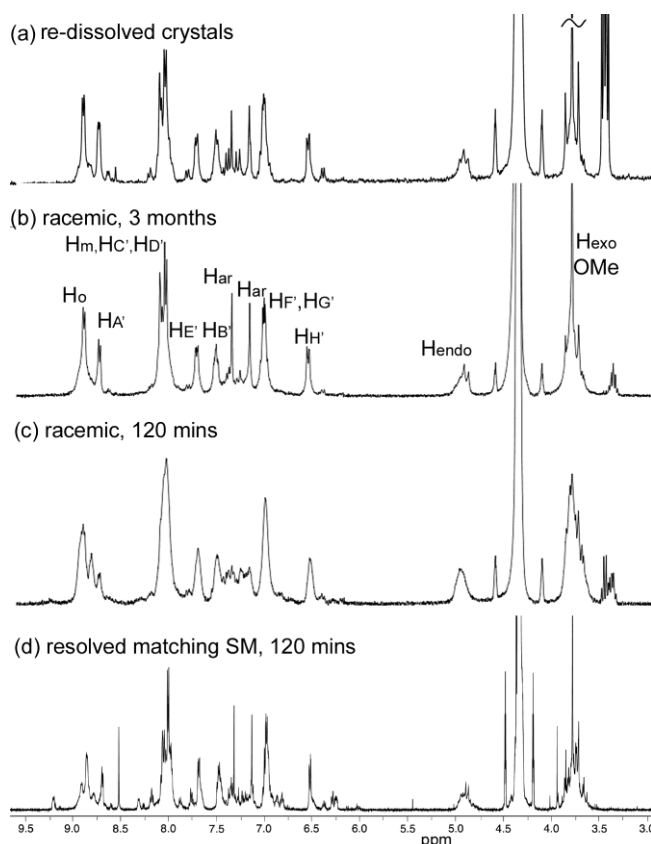


**Figure 2.** <sup>1</sup>H NMR spectra of cage **1** in CD<sub>3</sub>NO<sub>2</sub> of (a) re-dissolved racemic single crystals of *MM*- $\Lambda\Lambda\Lambda$  and *PP*- $\Delta\Delta\Delta$  cages of **1**·3BF<sub>4</sub>; (b) ( $\Lambda$ , $\Delta$ )-[Ir(ppy)<sub>2</sub>(MeCN)<sub>2</sub>]-PF<sub>6</sub> and ( $\pm$ )-L1 3 months after mixing; (c) ( $\Lambda$ , $\Delta$ )-[Ir(ppy)<sub>2</sub>(MeCN)<sub>2</sub>]-PF<sub>6</sub> and ( $\pm$ )-L1 two hours after mixing; (d) matched pair of  $\Delta$ -[Ir(ppy)<sub>2</sub>(MeCN)<sub>2</sub>]<sup>+</sup> and one L1 enantiomer after 2 hrs.

Homochiral metallo-cages with *tris*-chelate metal coordination are known both from achiral<sup>[13a-b]</sup> and resolved chiral ligands.<sup>[13c-e]</sup> Metallo-cages that show homochiral self-sorting from a racemic mixture of ligand enantiomers observed in solution are rare,<sup>[14]</sup> though include Pd(II) metallo-cryptophanes.<sup>[8a]</sup> The simultaneous chiral self-sorting of both ligand and pre-formed inert metallo-tecton as reported here has not been previously reported.

In a preliminary investigation of the influence of chiral guests on the self-assembly of cage **1** globular additives were included in 3:2 mixtures of ( $\Lambda$ , $\Delta$ )-[Ir(ppy)<sub>2</sub>(MeCN)<sub>2</sub>]-PF<sub>6</sub> and ( $\pm$ )-L1. Addition of chiral *R*-camphor or *S*-camphor led to noticeably faster sharpening of the <sup>1</sup>H NMR spectra than in their absence, but this was not observed for addition of achiral adamantane (Fig. S15-S20). Interestingly, addition of the related anionic species *R*-(*or S*)-10-camphorsulfonic acid to the reaction mixture prevents cage formation presumably as carboxylate is a competing ligand for the iridium (Fig. S21-22).

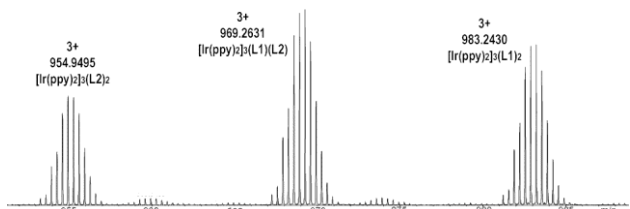
The cages do not show self-recognition of L-ligand species. ESI-MS of a MeNO<sub>2</sub> solution of L1, L2 and [Ir(ppy)<sub>2</sub>(MeCN)<sub>2</sub>]-BF<sub>4</sub> shows a statistical mixture of  $1:[\text{Ir}(\text{ppy})_2]_3(\text{L}1)(\text{L}2)]^{3+}:2$  cage species, Fig. 3. Mixing **1**·3BF<sub>4</sub> and **2**·3BF<sub>4</sub> in MeNO<sub>2</sub> results in very slow exchange between L1 and L2 with appreciable ligand

**Table 1.** Photophysical properties of complexes **1**-3(BF<sub>4</sub>) and **2**-3(BF<sub>4</sub>).

	$\lambda_{em}$ (nm)			$\Phi_{PL}$ (%) <sup>[d]</sup>			$\tau_e$ (ns) <sup>[g]</sup>		
	DCM [a,b,f]	film [c,f]	powder	DCM [a]	Film [c,e]	powd er [e]	DCM [a]	film [c]	powder
<b>1</b>	604	481 (0.7), 514 (1), 556 (0.8)	648	1	5.5	1.3	59 (0.7), 129 (0.3)	634 (0.4), 2319 (0.6)	55 (0.6), 203 (0.4)
<b>2</b>	485 (0.8), 516 (1), 547 (0.6)	486 (0.8), 515 (1), 545 (0.6)	519	15	10	1.6	523 (0.4), 887 (0.6)	688 (0.7), 3042 (0.3)	141 (0.4), 1175 (0.6)

[a] Measurements in degassed DCM at 298 K. [b] Quinine sulfate employed as the external reference ( $\Phi_{PL} = 54.6\%$  in 0.5 M H<sub>2</sub>SO<sub>4</sub> at 298 K). [c] PMMA doped films (5 wt % of cage) formed by spin-coating deposition on quartz substrate. [d]  $\Phi_{PL}$  measurements were carried out under nitrogen ( $\lambda_{exc} = 360$  nm). [e] values obtained using an integrating sphere. [f] Principal emission peaks listed with values in brackets indicating relative intensity. [g]  $\lambda_{exc} = 378$  nm; Values in parentheses are pre-exponential weighting factor, in relative % intensity, of the emission decay kinetics.

exchange only observed after 4 weeks, and near-statistical mixing reached after 10 weeks (Figure S6). Thus these cages have a high degree of kinetic stability but are not completely inert. It is interesting to note that this speciation behavior is in contrast with recently reported [Pd<sub>3</sub>L<sub>2</sub>]<sup>6+</sup> metallo-cryptophanes, which exclusively formed homocages from two different L-type ligands, with no ligand exchange.<sup>[8a]</sup>

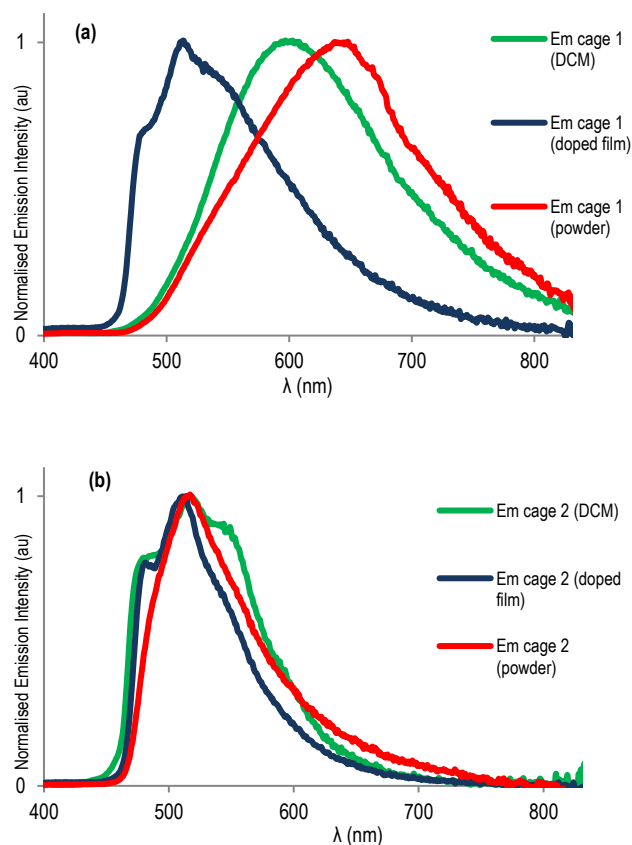
**Figure 3.** ESI-MS of a 1:1:3 mixture of L1:L2: [Ir(ppy)<sub>2</sub>(MeCN)<sub>2</sub>]<sup>+</sup>·BF<sub>4</sub> in MeNO<sub>2</sub> showing formation of statistical mixture of homoleptic and heteroleptic cages.

The absorption spectra of **1** and **2** in dichloromethane (DCM) are similar to other [Ir(ppy)<sub>2</sub>(N<sup>n</sup>N)]<sup>+</sup> systems,<sup>[7]</sup> and characterised by two intense ligand centered (<sup>1</sup>LC) transitions between 260 and 320 nm localised on the ppy and three lower intensity broad bands at below 380 nm that consist of spin-allowed and spin-forbidden mixed metal-to-ligand and ligand-to-ligand charge transfer (<sup>1</sup>MLCT/<sup>1</sup>LLCT and <sup>3</sup>MLCT/<sup>3</sup>LLCT) transitions (Fig. S26). The weak CT transition observed for **1** at 470 nm was not reported for the monomeric [Ir(ppy)<sub>2</sub>(4-pyCO<sub>2</sub>Et)<sub>2</sub>]<sup>+</sup> (4-pyCO<sub>2</sub>Et = 4-ethyl isonicotinate),<sup>[10c]</sup> pointing to increased conjugation in **1** due to the CTV scaffold. For both **1** and **2**, the excitation spectra in DCM match the absorption spectra and indicate a single photophysically-active species.

Cages **1** and **2** are emissive in DCM solution and in the solid state. Upon photoexcitation of **1**, a broad and unstructured emission is observed both in DCM and in the powder, Fig. 4a, due to emission from a mixed <sup>3</sup>MLCT/<sup>3</sup>LLCT state.<sup>[7]</sup> The photoluminescence spectrum in the powder is red-shifted ( $\lambda_{max} =$

648 nm) compared to that in DCM ( $\lambda_{max} = 604$  nm); however, **1** possesses similarly low  $\Phi_{PL}$  of around 1% and bi-exponential decay kinetics in both media, Table 1. Due to the increased conjugation into the CTV scaffold, cage **1** shows red-shifted emission and similar  $\Phi_{PL}$  compared to [Ir(ppy)<sub>2</sub>(4-pyCO<sub>2</sub>Et)<sub>2</sub>]<sup>+</sup> ( $\lambda_{max} = 560$  nm;  $\Phi_{PL} = 2\%$ ).<sup>[10c]</sup> Lusby's [[Ir(ppy)<sub>2</sub>]<sub>2</sub>(tcb)<sub>4</sub>]<sup>6+</sup> cage also showed red-shifted emission ( $\lambda_{max} = 575$  nm) when compared with the corresponding [Ir(ppy)<sub>2</sub>(NCPH)<sub>2</sub>]OTf complex ( $\lambda_{max} = 525$  nm); however, unlike for cage **1** and other Ir(ppy)<sub>2</sub> discrete supramolecular systems,<sup>[15]</sup> the  $\Phi_{PL}$  for the Lusby cage was enhanced compared with that of the mononuclear complex ( $\Phi_{PL} = 4\%$  cf.  $\Phi_{PL} < 1\%$ ).<sup>[4]</sup>

In order to mitigate non-radiative vibrational motion in the cage we spin-coated 5 wt % of **1** in polymethyl methacrylate (PMMA), which serves as an inert matrix. The emission in the thin film was blue-shifted and more structured ( $\lambda_{max} = 514$  nm) compared to both the powder and solution spectra. The  $\Phi_{PL}$  of 5.5% was enhanced as a result of the rigidification conferred by the PMMA host and the emission lifetimes were significantly longer ( $\tau_e = 634$  and 2319 ns).

**Figure 4.** Normalised photoluminescence spectra of a) **1**·3BF<sub>4</sub> and b) **2**·3BF<sub>4</sub>. Dotted lines de-aerated DCM solution; dashed lines PMMA doped films with 5 wt % of cages spin-coated on a quartz substrate; red lines bulk powders.

The photoluminescence spectrum of cage **2** in DCM is more structured and blue-shifted ( $\lambda_{max} = 516$  nm) compared to **1**, indicating emission that is more predominantly ligand-centered (<sup>3</sup>LC) (Fig. 4(b)). The blue-shifted emission of **2** compared to **1**

was expected considering the presence of the electron-withdrawing ester moieties located on L1 in **1**, which stabilise the LUMO.<sup>[10c]</sup> Cage **2** shows a significantly enhanced  $\Phi_{\text{PL}}$  and longer  $\tau_{\text{e}}$  compared to **1** in DCM ( $\Phi_{\text{PL}} = 15\%$ ,  $\tau_{\text{e}} = 523, 887 \text{ ns}$ ).

Unlike for **1**, as a powder the emission of **2** is not significantly red-shifted ( $\lambda_{\text{max}} = 519 \text{ nm}$ ) though the emission profile is less structured, showing less well-resolved vibrational bands as shoulders of the main emission peak. The emission profile for **2** in PMMA doped thin film is likewise very similar to that in DCM. Though  $\Phi_{\text{PL}}$  values are low in the powder ( $\Phi_{\text{PL}} = 1.6\%$ ), in doped film they are higher ( $\Phi_{\text{PL}} = 10\%$ ). Emission lifetimes are expectedly longer in doped films than in powder, Table 1. Attempts to synthesize an analogous mononuclear complex of 4-phenoxymethylpyridine for comparison were not successful due to ligand oligomerization.

In summary, phosphorescent  $[\{\text{Ir}(\text{ppy})_2\}_3(\text{L})_2]^{3+}$  metallo-cryptophanes can be synthesized in high yields, with the CTV-type ligands able to accommodate torsion angles typical of  $[\text{Ir}(\text{ppy})_2(\text{L})_2]$  complexes to form rare examples of 3-D Ir(III) cyclometallated coordination cages. These cages undergo ligand exchange processes over months, and show a remarkably high degree of homochiral self-sorting of both ligand and metallocenter, but not self-recognition between similar L-type ligands. Chiral sorting is enhanced by the presence of neutral chiral additives. For cage **1** chiral self-sorting occurs relatively rapidly upon crystallization through an induced seeding effect, but on a timescale of months in solution. Luminescence properties of the two cages are quite distinct, pointing to an ability to tune the photophysical properties of these systems. Cage **2** showed an enhanced and blue-shifted emission compared to **1**, reaching a  $\Phi_{\text{PL}}$  of 15% in DCM solution and 10% in doped film. These are promising systems for a variety of applications: as semiochemical hosts, photoredox catalysts and in energy conversion materials.

## Acknowledgements

We thank the EPSRC (DTG award 1238852, EP/K039202/1, EP/M02105X/1, EP/J001325/1), Leverhulme Trust (RPG-2014-148), University of St Andrews, and the MEXT/JSPS Grants in Aid for Scientific Research (JP25102005 and JP25102001) for funding; Simon Barrett for assistance with NMR; Martin Huscroft for assistance with HPLC, and Stephen Boyer for elemental analysis measurements.

**Data accessibility.** Data supporting this work can be accessed at DOI:#####.

**Keywords:** supramolecular chemistry; cage compounds • homochiral self-sorting • phosphorescence

- [1] Reviews: a) S. Zarra, D. M. Wood, D. A. Roberts, J. R. Nitschke, *Chem. Soc. Rev.* **2015**, *44*, 419-432; b) T. R. Cook, Y.-R. Zheng, P. J. Stang, *Chem. Rev.* **2013**, *113*, 734-777; c) K. Harris, M. Fujita, *Chem. Commun.* **2013**, *49*, 6703-6712; d) M. D. Ward, *Chem. Commun.* **2009**, 4487-4499; e) D. Fiedler, D. H. Leung, R. G. Bergman, K. N. Raymond, *Acc. Chem. Res.*, **2005**, *38*, 349-358.
- [2] for examples and reviews a) J. R. Piper, L. Cletheroe, C. G. P. Taylor, A. J. Metherell, J. A. Weinstein, I. V. Sazanovich, M. D. Ward, *Chem. Commun.* **2017**, *53*, 408-411; b) A. Schmidt, M. Hollering, M. Drees, A. Casini, F. E. Kühn, *Dalton Trans.* **2016**, *45*, 8556-8565; c) L. Xu, Y.-X. Wang, H.-B. Yang, *Dalton Trans.* **2015**, *44*, 867-890; d) X. Yan, T. R. Cook, P. Wang, F. Huang, P. J. Stang, *Nature Chem.* **2015**, *7*, 342-348; e) J. E. M. Lewis, A. B. S. Elliot, C. J. McAdam, K. C. Gordon, J. D. Crowley, *Chem. Sci.* **2014**, *5*, 1833-1843; f) Z. Li, N. Kishi, K. Yoza, M. Akita, M. M. Yoshizawa, *Chem. Eur. J.* **2012**, *18*, 8358-8365; g) K. Harano, S. Hiraoka, M. Shionoya, *J. Am. Chem. Soc.* **2007**, *129*, 5300-5301; h) N. K. Al-Rasbi, C. Sabatini, F. Barigelletti, M. D. Ward, *Dalton Trans.* **2006**, 4769-4772.
- [3] A. Schmidt, M. Hollering, J. Han, A. Casini, F. E. Kühn, *Dalton Trans.* **2016**, *45*, 12297-12300; b) A. B. S. Elliot, J. E. M. Lewis, H. van der Salm, C. J. McAdams, J. D. Crowley, K. C. Gordon, *Inorg. Chem.* **2016**, *55*, 3440-3447; c) W. J. Ramsay, J. A. Foster, K. L. Moore, T. K. Ronson, R. J. Mirgalet, D. A. Jefferson, J. R. Nitschke, *Chem. Sci.* **2015**, *6*, 7326-7331.
- [4] O. Chepelin, J. Ujma, X. Wu, A. M. Z. Slawin, M. B. Pitak, S. J. Coles, J. Michel, A. C. Jones, P. E. Barran, P. J. Lusby, *J. Am. Chem. Soc.* **2012**, *134*, 19334-19337.
- [5] a) X. Li, J. Wu, L. Chen, X. Zhong, C. Heng, R. Zhang, C. Duan, *Chem. Commun.* **2016**, *52*, 9628-9631; b) X. Li, J. Wu, C. Heng, R. Zhang, C. Duan, *Chem. Commun.* **2016**, *52*, 5104-5107.
- [6] a) C. Shen, A. D. W. Kennedy, W. A. Donald, A. M. Torres, W. S. Price, J. E. Beves, *Inorg. Chim. Acta.* **2017**, *458*, 122-128; b) J. Yang, M. Bhadbhade, W. A. Donald, H. Iranmanesh, E. G. Moore, H. Yan, J. E. Beves, *Chem. Commun.* **2015**, *51*, 4465-4468; c) A. B. Wragg, A. J. Metherell, W. Cullen and M. D. Ward, *Dalton Trans.* **2015**, *44*, 17939-17949; d) K. Li, L.-Y. Zhang, C. Yan, S.-C. Wei, M. Pan, L. Zhang, C.-Y. Su, *J. Am. Chem. Soc.* **2014**, *136*, 4456-4459.
- [7] a) D. R. Martir, A. K. Bansal, V. Di Mascio, D. B. Cordes, A. F. Henwood, A. M. Z. Slawin, P. C. J. Kamer, L. Martínez-Sarti, A. Pertegás, H. J. Bolink, I. D. W. Samuel, E. Zysman-Colman, *Inorg. Chem. Front.* **2016**, *3*, 218-235; b) A. M. Bünzli, E. C. Constable, C. E. Housecroft, A. Prescimone, J. A. Zampese, G. Longo, L. Gil-Escrig, A. Pertegás, E. Ortí, H. J. Bolink, *Chem. Sci.* **2015**, *6*, 2843-2852; c) S. Ladouceur, E. Zysman-Colman, *Eur. J. Inorg. Chem.* **2013**, 2985-3007; d) Y. You, S. Y. Park, *Dalton Trans.* **2009**, 1267-1282; e) S. Lamansky, P. Djurovich, D. Murphy, F. Abdel-Razzaq, H.E. Lee, C. Adachi, P. E. Burrows, S. R. Forrest, M. E. Thompson *J. Am. Chem. Soc.* **2001**, *123*, 4304-4312.
- [8] a) A. Schaly, Y. Rousselin, J.-C. Chambron, E. Aubert, E. Espinosa, *Eur. J. Inorg. Chem.* **2016**, 832-843; b) J. J. Henkels, C. J. Carruthers, S. E. Chambers, R. Clowes, A. I. Cooper, J. Fisher, M. J. Hardie, *J. Am. Chem. Soc.* **2014**, *136*, 14393-14396; c) Z. Zhong, A. Ikeda, S. Shinkai, S. Sakamoto, K. Yamaguchi, *Org. Lett.* **2001**, *3*, 1085-1087.
- [9] CCDC 1486233 contain the supplementary crystallographic data for this paper. These data are provided free of charge by The Cambridge Crystallographic Data Centre.
- [10] a) C.-T. Wang, L.-C. Shiu, K.-B. Shiu *Chem.-Eur.J.* **2015**, *21*, 7026-7029; b) V. Chandrasekhar, T. Hajra, J. K. Bera, S. M. W. Rahaman, N. Satumtira, O. Elbejrani, M. A. Omary, *Inorg. Chem.* **2012**, *51*, 1319-1329; c) E. Baranoff, I. Jung, R. Scopelliti, E. Solari, M. Gratzel, Md. K. Nazeeruddin, *Dalton Trans.* **2011**, *40*, 6860-6867; d) W.-S. Sie, G.-H. Lee, K. Y.-D. Tsai, I.-J. Chang, K.-B. Shiu, *J. Mol. Struct.* **2008**, *890*, 198-202.
- [11] While NMR spectra of ( $\pm$ )-L1 remain unchanged with time, small additional peaks appear in the  $^1\text{H}$  NMR spectra of  $\text{CD}_3\text{NO}_2$ -solutions of resolved L1 at room temperature (Fig. S2). This may be due to an unknown minor decomposition or saddle-like conformation from crown-saddle-crown racemisation, see for example G. Huber, T. Brotin, L. Dubois, H. Desvaux, J.-P. Dutasta, P. Berthault, *J. Am. Chem. Soc.* **2006**, *128*, 6239-6246.
- [12] J. J. Henkels, J. Fisher, S. L. Warriner, M. J. Hardie, *Chem. -Eur. J.* **2014**, *20*, 4117-4125.
- [13] a) P. Bonakdarzadeh, F. Pan, E. Kalenius, O. Jurček, K. Rissanen, *Angew. Chem. Int. Ed.* **2015**, *54*, 1480-14893; b) D. L. Caulder, R. E. Powers, T. N. Parac, K. N. Raymond, *Angew. Chem. Int. Ed.* **1998**, *37*,

- 
- 1840-1843. c) J. L. Bolliger, A. M. Belenguer, J. R. Nitschke, *Angew. Chem. Int. Ed.* **2013**, *52*, 7958-7962; d) T. Liu, Y. Liu, W. Xuan, Y. Cui, *Angew. Chem. Int. Ed.* **2010**, *49*, 4121-4124; e) S. P. Argent, T. Riis-Johannessen, J. C. Jeffery, L. P. Harding, M. D. Ward, *Chem. Commun.* **2005**, 4647-4649.
- [14] a) S. A. Boer, D. R. Turner, *Chem. Commun.* **2015**, *51*, 17375-17378; b) L.-L. Yan, C.-H. Tan, G.-L. Zhang, L.-P. Zhou, J.-C. Bünzli, Q.-F. Sun, *J. Am. Chem. Soc.* **2015**, *137*, 8550-8555; c) C. Gütz, R. Hovorka, G. Schnakenburg, A. Lützen, *Chem. Eur. J.* **2013**, *19*, 10890-10894; d) C. Maeda, T. Kamada, A. Osuka, *Chem. Soc. Rev.* **2007**, *251*, 2743-2752.
- [15] E. Baranoff, E. Orselli, L. Allouche, D. Di Censo, R. Scopelliti, M. Grätzel, M. K. Nazeeruddin, *Chem. Commun.* **2011**, *47*, 2799-2801.
-

---

---